Article

Improving Deep Learning-Based UWB LOS/NLOS Identification with Transfer Learning: An Empirical Approach

JiWoong Park [1], **SungChan Nam** [2], **HongBeom Choi** [1], **YoungEun Ko** [2] and **Young-Bae Ko** [1,2,*]

[1] Department of AI Convergence Network, Ajou University, Suwon 16499, Korea; z7080z@ajou.ac.kr (J.P.); credtiger96@ajou.ac.kr (H.C.)

[2] Department of Software and Computer Engineering, Ajou University, Suwon 16499, Korea; skdiakffn@ajou.ac.kr (S.N.); kye0420@ajou.ac.kr (Y.K.)

* Correspondence: youngko@ajou.ac.kr; Tel.: +82-031-219-1841

check for updates

Abstract: This paper presents an improved ultra-wideband (UWB) line of sight (LOS)/non-line of sight (NLOS) identification scheme based on a hybrid method of deep learning and transfer learning. Previous studies have limitations, in that the classification accuracy significantly decreases in an unknown place. To solve this problem, we propose a transfer learning-based NLOS identification method for classifying the NLOS conditions of the UWB signal in an unmeasured environment. Both the multilayer perceptron and convolutional neural network (CNN) are introduced as classifiers for NLOS conditions. We evaluate the proposed scheme by conducting experiments in both measured and unmeasured environments. Channel data were measured using a Decawave EVK1000 in two similar indoor office environments. In the unmeasured environment, the existing CNN method showed an accuracy of approximately 44%, but when the proposed scheme was applied to the CNN, it showed an accuracy of up to 98%. The training time of the proposed scheme was measured to be approximately 48 times faster than that of the existing CNN. When comparing the proposed scheme with learning a new CNN in an unmeasured environment, the proposed scheme demonstrated an approximately 10% higher accuracy and approximately five times faster training time.

1. Introduction

Recently, ultra-wideband (UWB) technology has been adopted as the new wireless technology for smart keys [1]. Major smartphone manufacturers such as Samsung and Apple included UWB technology in their latest flagship smartphone models (iPhone 11 Pro and Galaxy Note 20 Ultra) [2]. According to this trend, a new standard for UWB wireless communication, called IEEE 802.15.4z, was approved to improve ranging, robustness, and security [3]. UWB technology has significant advantages in localization owing to its centimeter-level ranging capability, multipath robustness, and low energy consumption [4,5]. UWB is considered as the most promising technology for accurate positioning, which is required for various applications such as the Internet of Things (IoT), wearable devices, extended reality (XR), sports training, maritime communication, future wireless networking, and unmanned aerial robots [6–13]. For example, in XR applications, if an object's location is incorrectly displayed, the user experience (UX) is significantly degraded. To meet these demands, research to improve the accuracy of UWB ranging is essential.

The non-line of sight (NLOS) condition is usually referred to as the most influential factor in the deterioration of UWB ranging performance [14]. The NLOS condition refers to a situation where an obstacle is placed between the transmitter and the receiver. In this case, the signal is propagated by penetrating the obstacles or being reflected on indirect paths. The NLOS ranging error is included in both cases when penetrating obstacles or traveling longer distances. In a real environment, there may be many NLOS conditions for walls, desks, pedestrians, computers, and so on. To solve the NLOS error, it is crucial to first identify the LOS/NLOS signals.

Studies are being conducted to identify LOS/NLOS signals. The most recent studies have attempted to analyze UWB channel measurements such as the channel impulse response (CIR) for LOS/NLOS identification. As the radio signal penetrates through obstacles or reflects, the amplitude decreases and a delay occurs, which is reflected in the CIR. Channel-based NLOS identification methods detect these features by analyzing the CIR. A number of studies have applied machine learning to identify NLOS conditions using channel data. However, previous machine learning-based schemes have a critical limitation, in that they show significant performance degradation in places where training is not taking place. This is because the UWB channel is not only influenced by obstacles, but also by the surrounding environment. Since environmental noise is included in the training data, the classification model also learns environmental noise. The classification accuracy is degraded when processing data are measured in places with different patterns of environmental noise. Therefore, using machine learning-based LOS/NLOS identification schemes in unknown places is a challenge. To use existing methods in an unknown environment, a new model for the environment is required. Training a new model for a new place requires considerable time in the data collection and learning process. To deal with these problems, we propose a UWB NLOS identification scheme based on a neural network and transfer learning. To the best of our knowledge, this is the first study on empirically analyzing the problem of UWB NLOS identification accuracy degradation in an unmeasured environment and proposing a transfer learning-based solution. The main contributions of this paper are as follows:

- We introduce two UWB channel classification schemes based on multilayer perceptron (MLP) and convolutional neural network (CNN).
- We propose a transfer learning algorithm for accurate NLOS classification in an unmeasured place.
- We conduct extensive experiments using commercial UWB devices to examine the performance of a deep neural network (DNN) model in an unmeasured environment.
- By comparing the performance, we propose a model for optimizing the neural network structure according to the surrounding environment. In this model, we implement a transfer learning-based NLOS condition classification method for an unmeasured environment.

The remainder of this paper is organized as follows. Section 2 introduces related works for UWB NLOS identification. In Section 3, the UWB NLOS identification scheme is proposed. In Section 4, the experimental setup is introduced. In Section 5, we analyze experiments and evaluate the result. In Section 6, we conclude our work, and future works are discussed.

2. Related Work

To improve the accuracy of indoor positioning, several methods for LOS/NLOS identification have been discussed from various perspectives. In this paper, we focused on the channel-based technique and divide the studies into two categories: algorithm-based classification and machine learning-based classification. The first category of studies devises an algorithm for identifying NLOS. The second category uses machine learning techniques to extract features or identify NLOS. Since the proposed scheme is based on machine learning, we focus more on the latter.

2.1. Algorithm-Based NLOS Identification

Algorithm-based schemes extract meaningful features from channel measurement and devise an algorithm for identifying NLOS. Yu et al. [15] proposed an NLOS identification algorithm based on the

total energy, maximum amplitude, normalized strongest path energy, signal-to-noise ratio, rise time, kurtosis, and mean excess delay. The optimal feature combination was found through the Pearson correlation coefficient, and multiple obstacles were detected through a fuzzy comprehensive evaluation. Kim et al. [16] separated the first path signal and the multipath signal from channel data and compared them for NLOS identification. The NLOS detection algorithm based on the particle filter was discussed in [17]. In [18], an algorithm for identifying the NLOS by comparing the received signal strength and first path power strength was proposed. These algorithm-based schemes are simple enough to operate in low-cost UWB devices. However, most algorithms use environment-dependent constants as the threshold value to classify NLOS conditions. Finally, the identification performance is not promising.

2.2. Machine Learning-Based NLOS Identification

There are two approaches to identify NLOS conditions using machine learning. The first one uses human-extracted features as the input for machine learning. Eighteen features were extracted from the CIR data, and a genetic algorithm found the best feature combination for NLOS identification [19]. The selected features were used as input data for a support vector machine (SVM). Kristensen et al. [20] also used SVM as a classifier model. Linear discriminant analysis was used to train the model. The received signal strength (RSS) and ranging value were used as inputs for the SVM to identify the NLOS signals [21]. The researchers targeted low-cost devices that cannot measure high-resolution channel data. These SVM-based classification methods show high classification performance with relatively small amounts of training data. However, as the amount of training data increases, the identification performance of SVM-based methods decreases significantly. A K-means clustering-based LOS/NLOS identification scheme was proposed in [22]. The mean excess delay, kurtosis, and root mean squared delay spread were used as inputs for training. Fan et al. [23] applied unsupervised learning based on Gaussian mixture models to the LOS/NLOS identification problem. Since both methods use unsupervised learning, they have the advantage that models can be trained using label-less data. However, the classification accuracy is relatively low. The second method extracts the features from neural networks so that all of the channel data are used as the input for machine learning. Wang et al. [24] proposed the LOS/NLOS identification method based on a CNN image classification model. After storing the CIR data in the form of an image using a short-time Fourier transform, they were used as the input data for the CNN to train the model. The researchers successfully transformed the NLOS identification problem into the form of image classification. Three types of CNN architecture (ResNet, encoder, and fully connected network) were applied to detect NLOS channel conditions [25]. Raw CIR data were used as the input for each CNN. By comparing the performance of the three CNN architectures, it was proven that there was little of a relationship between the CNN architecture and NLOS detection performance. ShirinAbadi et al. [26] proposed a CNN-based LOS/NLOS identification scheme using CIR data. To address the sparsity phenomenon, two cost functions for the UWB NLOS problem were defined. In the experiment, the effectiveness of the number of convolution layers was investigated. These CNN-based schemes showed higher classification accuracies than other machine learning-based approaches. However, the classification performance deteriorated in places where the training data were not sufficiently collected. Jiang et al. [27] proposed a long short-term memory (LSTM)-based UWB channel classification scheme. To effectively learn the long-range dependencies of the time-series data of the UWB CIR data, the fully connected layer of the CNN was replaced by an LSTM layer. However, there is no distinct difference in the performance of CNN-based approaches.

Most neural network-based methods show high performance in measured environments, but they do not consider unmeasured environments. Channel measurement includes not only characteristics owing to obstacles, but also characteristics owing to environmental noise generated by the surrounding environment. If the NLOS identification model tries to classify the data from an unmeasured environment even with the same obstacles, the performance may be severely degraded. The existing neural network-based methods do not consider the problems caused by this unmeasured environment. In existing schemes, a new model should be trained in an unmeasured environment. However,

training a new model for a new place requires a significant amount of data to be collected and is time consuming. To solve this problem, we propose a UWB NLOS identification scheme based on transfer learning for an unmeasured environment. Transfer learning can update existing models to fit the new environment with few data items and a short training time.

3. UWB NLOS Identification

In this section, we first analyze the problems occurring in an unmeasured environment through UWB channel models and experiments. Then, two kinds of neural network architectures are described for the NLOS classifier. The proposed transfer learning scheme is described to quickly update the neural network model to the unmeasured environment.

3.1. Problem Statement

The CIR of a UWB can be represented using the Saleh–Valenzuela model [28]:

$$h(t) = \sum_{l=0}^{L} \sum_{k=0}^{K} a_{k,l} \exp(\phi_{k,l}) \delta(t - T_l - \tau_{k,l}), \tag{1}$$

where $a_{k,l}$ is the weight of the k-th component in the l-th cluster, T_l is the delay of the l-th cluster, $\tau_{k,l}$ is the delay of the k-th multipath component relative to the l-th cluster arrival time, and $\phi_{k,l}$ is the phase of the k-th component in the l-th cluster. To consider multipath effects, the number of clusters, **L**, is modeled as a Poisson distribution.

$$pdf_L(L) = \frac{(\bar{L})^L \exp(-\bar{L})}{L!} \tag{2}$$

assuming that the $\bar{L}$ number of clusters arrives at the receiver, the ray arrival time of the l-th cluster is presented as follows:

$$p(\tau_{k,l}|\tau_{(k-1),l}) = \lambda_i \exp[-\lambda_i(\tau_{k,l} - \tau_{(k-1),l})], \tag{3}$$

where λ_i is the cluster arrival rate of the i-th cluster. To model a complex environment, a mixture model that is a weighted summation of several ray arrival time models can be used. The power delay profile of the k-th component in the l-th cluster is presented as:

$$E\{|a_{k,l}|^2\} = \Omega_l \frac{1}{\gamma_l[\lambda_i + 1]} \exp(-\tau_{k,l}/\gamma_l), \tag{4}$$

where Ω_l is the integrated energy of the l-th cluster and γ_l is the intracluster decay time constant. In the case of the NLOS environment, the power delay profile of the k-th component in the l-th cluster is different:

$$E\{|a_{k,l}|^2\} = (1 - \chi \exp(-\tau_{k,l}/\gamma_{rise})) \exp(-\tau_{k,l}/\gamma_1) \frac{\gamma_1 + \gamma_{rise}}{\gamma_1} \frac{\Omega_1}{\gamma_1 + \gamma_{rise}(1 - \chi)}, \tag{5}$$

where χ is the attenuation of the first component, γ_{rise} determines how fast the power delay profile increases to its local maximum, and γ_1 determines the decay at late times. In the UWB channel model, many environment-dependent constants are involved in the CIR. The number of clusters, cluster arrival rate, and power of the cluster vary depending on the environment. In Equation (5), it can be seen that the environment-dependent constant is involved in a large part of the power delay profile even under the NLOS condition. The impulse response changes more significantly in NLOS than in LOS owing to γ_{rise} and γ_1 by Equation (5). Even in a similar environment, small differences can cause significant differences in the CIR.

To confirm this channel model-based analysis in an actual environment, an experiment was performed to collect the CIR in similar spaces. Figure 1 shows the CIR of UWB signals with the same

obstacles in similar spaces (the experimental setup is described in Section 4). The two spaces where the CIRs were measured had similar environmental features that could be expressed as an indoor office. Although both signals penetrated the same obstacle in a similar environment, a completely different CIR was measured because of the environmental noise generated in each place. If the machine learning-based NLOS identification method trains the data as in Figure 1a and tries to classify the signal as in Figure 1b, then the classification performance may be seriously degraded. Thus, it is necessary to study an NLOS identification scheme for an unmeasured environment.
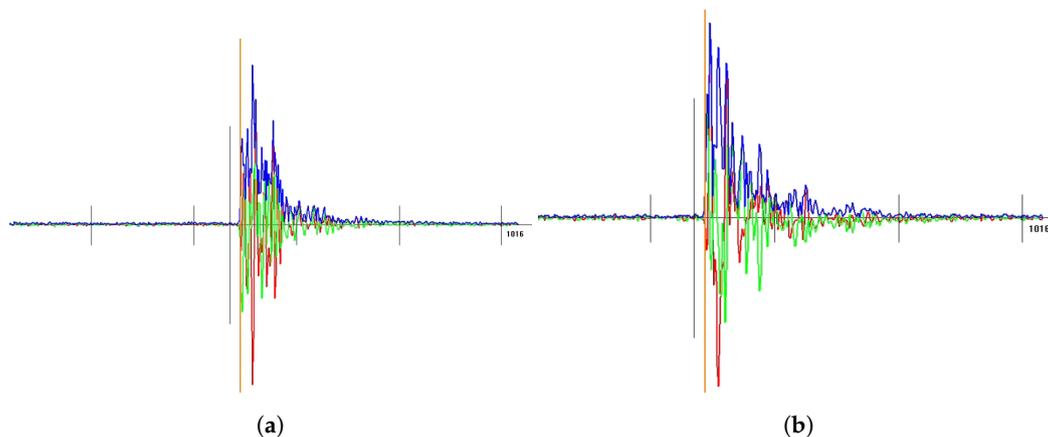

| (a) | (b) |

Figure 1. Signal waveform measured in two different places with the same obstacle: (**a**) laboratory; (**b**) classroom.

3.2. Proposed Scheme

The proposed UWB NLOS identification scheme consists of a learning phase and an update phase. In the learning phase, a neural network model is trained using a large amount of UWB channel data collected in advance. UWB channel data should be labeled with UWB channel conditions such as LOS and NLOS. We introduce two types of neural network architectures, MLP and CNN, as classifiers for the proposed scheme. The update phase begins in the unmeasured environment where NLOS identification is required. After collecting a small amount of data for a while, the existing neural network model is updated through transfer learning. After a short transfer learning process, an updated model will identify the UWB NLOS condition from the measured data. Next, the proposed scheme is explained in detail with a description on the structure of neural networks and the transfer learning method.

To classify NLOS conditions from the one-dimensional form of channel data, we used MLP and CNN structures. MLP is a widely used neural network-based classifier that shows good performance on single-dimensional time-sequential data such as speech recognition. Since UWB wireless channel measurement is also based on single-dimensional time-sequential data, we believe that MLP can perform well for the UWB NLOS identification problem. An MLP is composed of the input, hidden layer, and output, as illustrated in Figure 2a. In the hidden layer, the neural nodes of the previous layer are fully connected to the neural nodes of the next layer. The weight gradients are updated as the input data are propagated in the hidden layer. There is no feature extraction process in the MLP-based scheme. Our intention is to investigate the impact of feature extraction in the UWB NLOS identification problem. A CNN consists of an input, a convolution layer, a pooling layer, a hidden layer, and an output, as shown in Figure 2b. The input, hidden layer, and output are similar to those of the MLP. In a convolutional layer, features are extracted from the input with multiple kernel filters. After the feature extraction process takes place in the convolution layer, the downsampling process is performed in the pooling layer. A pooling layer minimizes the training computation and time. A major difference between the MLP and CNN is the feature extraction process. By analyzing the experimental results, we can confirm the impact of the feature extraction process in optimizing the neural network for the UWB NLOS identification problem.
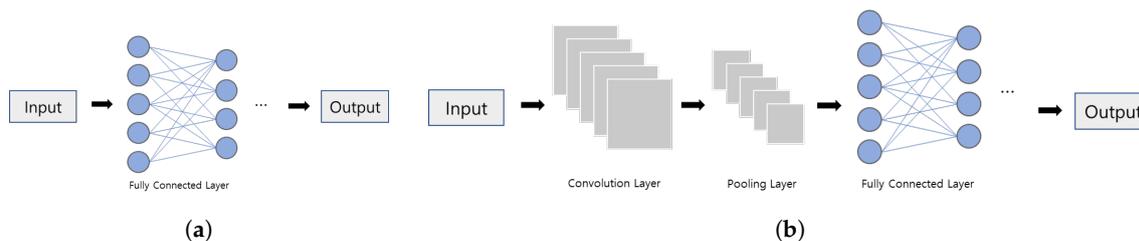
Figure 2. Neural network structure. (**a**) MLP; (**b**) CNN.

Transfer learning is usually adopted when solving a related problem with an existing model. We believe that the UWB NLOS identification problem at different places can be considered as an example. When the signal measuring place changes, it can be implied that the problem has also changed with environmental noise. However, it can also be implied that the two problems are related to each other because they have common obstacles. We want to identify the UWB NLOS condition in an unmeasured environment with the existing "trained model" for speed and accuracy. To apply the transfer learning concept to our proposed classifiers, we selected a weight initialization method called fine-tuning, as shown in Figure 3. The weight gradients of the last hidden layer are initialized to zero and retrain the neural network with a few unmeasured environment data. While the neural network is recovering weight gradients, the characteristics of unmeasured environment data are reflected in the neural network. Because only the last layer of weight gradients is initialized, the training requires a relatively small amount of data and time. When applying transfer learning to an MLP, it is necessary to set some hidden layers as non-trainable layers to maintain the previous knowledge.
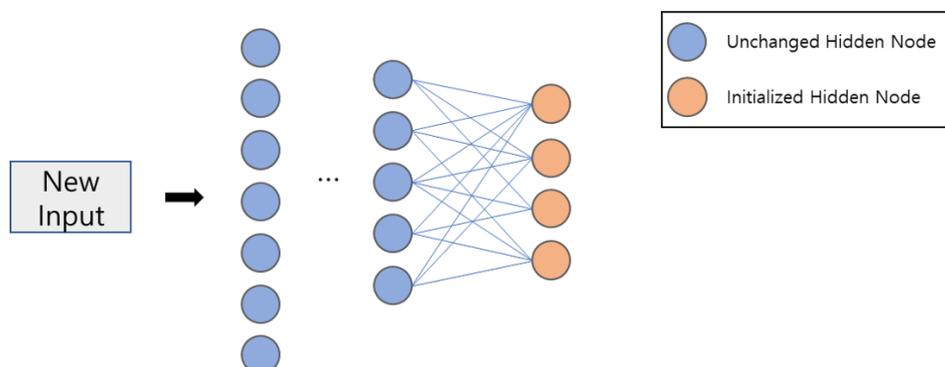

Figure 3. Transfer learning concept used in the proposed scheme.

4. Experimental Setup

The UWB CIR data were measured in the iCONS Lab and in a classroom in Paldal Hall, Department of Computer Engineering, Ajou University, Korea (see Figure 4). Both places represent examples of an indoor office environment by containing similar obstacles including iron doors, concrete walls, desks, chairs, pedestrians, and computers. In this experiment, we divide the channel condition into three categories: (1) LOS, (2) weak NLOS, and (3) NLOS. In the LOS condition, signals are propagated in the shortest distance without interference from obstacles. The weak NLOS condition indicates that the signal is obstructed by small obstacles such as pedestrians, monitors, and desks. The NLOS condition implies that concrete walls or iron doors obstruct the signal. To increase data diversity, we collected 3100 data each for LOS, weak NLOS, and NLOS in each room. While collecting the data, we changed the location of the devices to diversify the environmental noise and distance. In total, three-thousand data items were used for training a neural network, and one-hundred data items were used for transfer learning. The collected data were randomly divided into training data, validation data, and test data at a 6:2:2 ratio. In summary, we collected a total of 9300 data items (3000 LOS data, 3000 weak NLOS data, 3000 NLOS data, 100 LOS data for transfer learning, 100 weak

NLOS data for transfer learning, and 100 NLOS data for transfer learning) for both the lab and classroom environments.
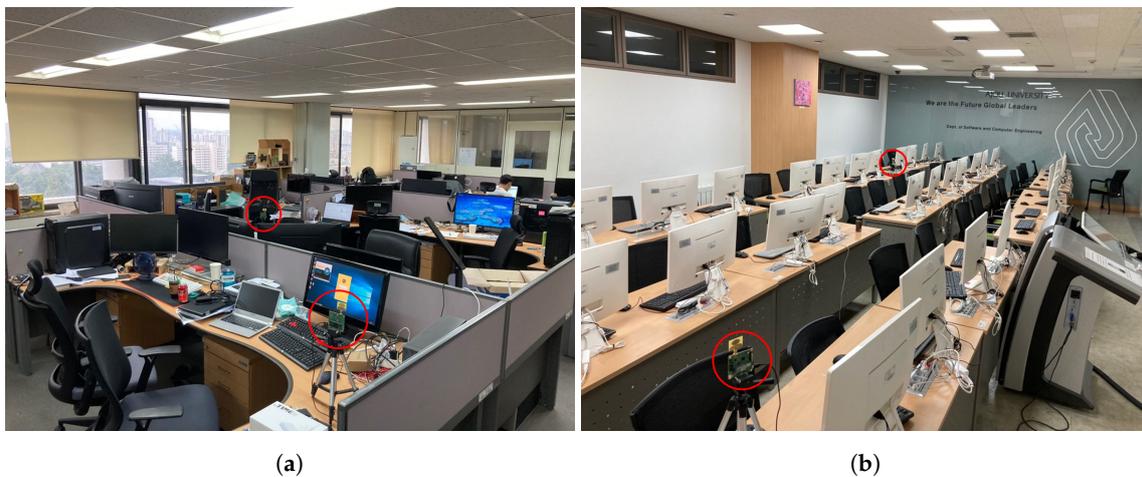
Figure 4. Two rooms in Paldal Hall, Ajou University, used for measuring the UWB channel. (**a**) Laboratory located on the ninth floor of the building; (**b**) classroom located on the third floor.

The Decawave EVK1000 Evaluation Kit was used in UWB CIR data measurement [29]. The EVK 1000 provides a ranging function that complies with the IEEE802.15.4-2011 UWB standard and provides an application programming interface (API) that can collect wireless channel data such as CIR in real time. The collected UWB CIR data consist of 1016 real parts of signals and 1016 imaginary parts. Each pair of real and imaginary parts of signals is measured once every nanosecond. The channel setting of the transceiver had a data rate of 110 kb/s, central frequency of 4.0 GHz, preamble length of 1024, and pulse reception frequency of 64 MHz. The proposed neural network models were implemented on an Ubuntu 18.04 workstation with i9-7940x CPU (3.10 GHz), 128 GB RAM, 2 GTX 1080Ti scalable link interface (SLI) GPUs, and a 1 TB solid state drive (SSD).

We optimized the neural network structures through iterative experiments for this experimental setup. If the size of the input or output is changed, then the structure of the neural network needs to be optimized again. The MLP has an input layer consisting of 2032 nodes, 3 fully connected layers (also called dense) consisting of 128 nodes, and a fully connected layer consisting of 3 nodes. The CNN has the same input and output layer, but it has two convolution layers and a pooling layer added between the input layer and the fully connected layers. For neural network model training, the Adam optimizer, the categorical cross entropy loss function, and the accuracy classification metric were used. The detailed network setups for the MLP are shown in Table 1, and those for the CNN are shown in Table 2. In the transfer learning learning process, we set all layers to be untrainable except for the last two dense layers. For MLP, only dense_2 and dense_3 layers were set to trainable, and for CNN, only dense_1 and dense_2 were set to be trainable.

Table 1. Neural network layer configuration information of the MLP used in the experiment.

Layer (Type)	Shape	Parameters
input (InputLayer)	2032	0
dense (Dense)	128	260,224
dense_1 (Dense)	128	16,512
dense_2 (Dense)	128	16,512
dense_3 (Dense)	3	387

Table 2. Neural network layer configuration information of the CNN used in the experiment.

Layer (Type)	Shape	Parameters
input (InputLayer)	2032	0
reshape (Reshape)	(2032, 1)	0
conv1d_1 (Conv1D)	(2025, 128)	1152
conv1d_2 (Conv1D)	(2018, 128)	131,200
max_pooling1d_1 (MaxPooling1D)	(1009, 128)	0
conv1d_3 (Conv1D)	(1002, 128)	131,200
conv1d_4 (Conv1D)	(995, 128)	131,200
max_pooling1d_2 (MaxPooling1D)	(497, 128)	0
flatten (Flatten)	63,616	0
dense (Dense)	128	8,142,976
dense_1 (Dense)	128	16,512
dense_2 (Dense)	3	387

5. Experimental Analysis and Performance Evaluation

We trained the MLP and CNN with lab and classroom data, respectively. Afterward, transfer learning was applied to each model. We evaluated the performance by comparing them in terms of the classification accuracy and computational overhead. Classification performance is presented in terms of accuracy, precision, and recall. Accuracy represents the comprehensive classification performance, and precision and recall represent each propagation condition's identification performance. Accuracy is calculated by dividing the true identification by all identification attempts. Precision is calculated by dividing the true positives by the predicted positives. Recall is calculated by dividing the true positives by the sum of false negatives and true positives. We measured the time for training the model to evaluate the computational overhead. In previous works, there was no neural network-based NLOS identification scheme for an unmeasured environment. Therefore, for performance evaluation of the proposed scheme, we compared the MLP and CNN with transfer learning to the MLP and transfer learning to the CNN. To compare the performance of updating an existing model and training a new model, we compared transfer learning to a light CNN. Light CNN refers to a CNN model newly trained with the same data used in transfer learning.

5.1. UWB Channel Classification Performance

To evaluate the UWB channel classification performance, we conducted experiments in a measured environment and an unmeasured environment. The unmeasured environment indicates that the training data and test data are extracted from different places, and the measured environment indicates the opposite. If we evaluate the MLP model trained with the lab data, the measured environment is the lab, and the unmeasured environment would be the classroom. The lab and classroom are alternately set as the measured and unmeasured environments.

5.1.1. Classification Performance in the Measured Environment

Figure 5 shows the UWB channel classification accuracy of the MLP and CNN in a measured environment. When comparing the CNN and MLP, the CNN always shows higher classification performance than the MLP. In particular, the CNN shows a high accuracy of over 97% in both places. With this result, we prove that the feature extraction process is effective for UWB NLOS identification. When comparing the classification performance according to the place, the classroom shows higher performance than the lab. This is because the lab environment has more obstacles, as shown in Figure 4. A complex lab environment produces environmental noise and degraded classification performance. In addition, the accuracy of the CNN decreases by approximately 1%, while the accuracy of the MLP decreases by approximately 4%. It is interpreted that the more severe the environmental noise, the greater the effect of the feature extraction process. Table 3 shows the precision and recall

of each UWB channel condition for the MLP and CNN in a measured environment. In the measured environment, the classification performances according to channel conditions are almost similar.
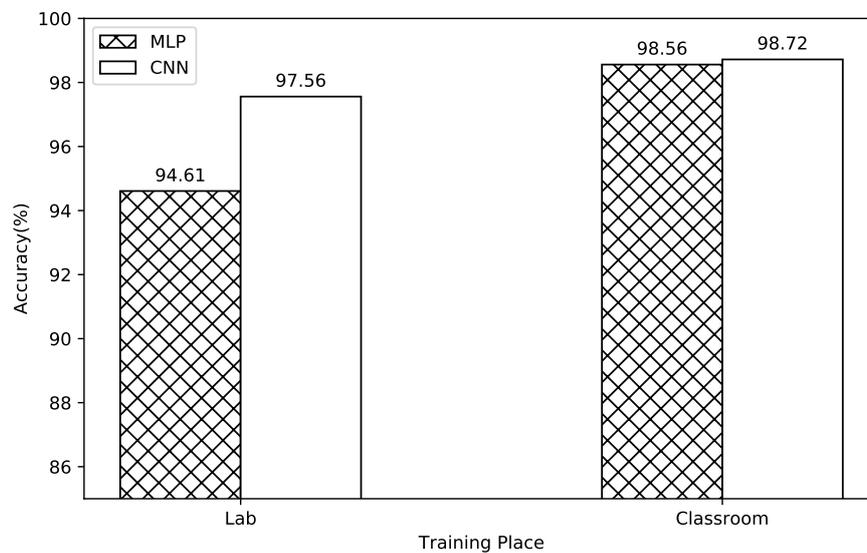

Figure 5. UWB channel classification accuracy of the MLP and CNN in the measured environment.

Table 3. UWB channel classification performance on the MLP and CNN in the measured environment.

	Train: Lab, Test: Lab				Train: Classroom, Test: Classroom			
	MLP		CNN		MLP		CNN	
	Precision	Recall	Precision	Recall	Precision	Recall	Precision	Recall
LOS	94.54	95.33	98.32	97.66	99.33	98.50	97.24	100.0
Weak NLOS	95.94	90.67	98.31	97.00	98.66	98.33	99.16	98.33
NLOS	93.47	97.84	96.08	98.00	97.69	98.33	99.83	97.83

5.1.2. Classification Performance in the Unmeasured Environment

Figure 6 compares the classification accuracy of the MLP, CNN, transfer learning to MLP, and transfer learning to CNN in an unmeasured environment. Classification models without transfer learning show significantly degraded accuracy in an unmeasured environment. Compared to the trained place experiment, the accuracy decreased by more than 50% in all cases. This is because environmental noise in each place is learned together during the training process. When transfer learning is applied, the classification accuracy increases up to 98%, which is almost the same as that of the measured environment. This result verifies that transfer learning can effectively eliminate the environmental noise contained in the existing model. When comparing the accuracy of transfer learning to the MLP and CNN, the CNN shows higher accuracy in every place. This shows that the feature extraction process is also crucial in transfer learning. Comparing the accuracy of transfer learning to MLP in different places, it can be seen that the classroom has a 15% higher accuracy than the lab. We deduce from this that transfer learning requires a feature extraction process in a complex environment. MLP shows higher accuracy without transfer learning in an unmeasured environment. This is because many environmental noises were included in the model during the CNN feature extraction process.

Tables 4 and 5 show the detailed UWB channel classification performance of the MLP, CNN, transfer learning to the MLP, and transfer learning to the CNN in an unmeasured environment. Without transfer learning, NLOS shows a significantly low recall of less than 8% in all cases. This means that the characteristics of environmental noise are mostly similar to those of NLOS.
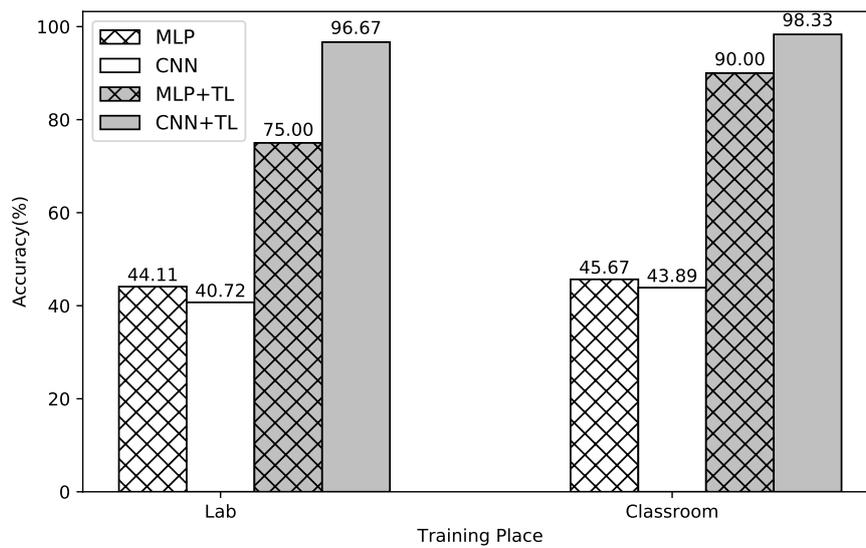
Figure 6. UWB channel classification accuracy of different training places and models.

Table 4. UWB channel classification performance of the MLP and CNN in different unmeasured environments.

| | Train: Lab, Test: Classroom | | | | Train: Classroom, Test: Lab | | | |
| | MLP | | CNN | | MLP | | CNN | |
	Precision	Recall	Precision	Recall	Precision	Recall	Precision	Recall
LOS	50.40	63.67	44.52	44.67	71.52	54.83	52.99	69.50
Weak NLOS	40.15	62.84	41.77	76.17	36.07	74.60	40.09	56.67
NLOS	33.98	5.83	7.69	1.33	45.92	7.50	20.00	5.50

Table 5. UWB channel classification performance of transfer learning to the MLP and transfer learning to the CNN in different unmeasured environments.

| | train: Lab, Test: Classroom | | | | Train: Classroom, Test: Lab | | | |
| | MLP+TL | | CNN+TL | | MLP+TL | | CNN+TL | |
	Precision	Recall	Precision	Recall	Precision	Recall	Precision	Recall
LOS	100.0	70.00	95.24	100.0	100.0	80.00	100.0	95.00
Weak NLOS	77.78	70.00	95.24	100.0	85.71	90.00	100.0	100.0
NLOS	60.71	85.00	100.0	90.00	86.96	100.0	95.24	100.0

Figure 7 shows the UWB channel classification accuracy of the light CNN and transfer learning to the CNN. In this experiment, we compared the performance of transfer learning and the CNN with the same amount of training data. Transfer learning shows over 98% accuracy, while the light CNN shows only approximately 88% accuracy. This is because the light CNN used inadequate training data, which caused the accuracy to become lower than the trained place accuracy presented in Section 5.1.1. Through these results, we prove that it is more efficient to use the existing CNN model with transfer learning than to train a new CNN model in an unmeasured environment.

5.2. Computational Overhead

Table 6 shows the training time of the MLP, CNN, transfer learning on MLP, transfer learning on CNN, and light CNN. The CNN requires 200 times more time for training than the MLP. This is because the convolution layers and pooling layers in a CNN require massive parallel computation. Transfer learning to the CNN only takes 7 s for training lab data. This is more than nine times faster than the CNN trained with the same amount of data and 48 times faster than the CNN that shows

similar classification accuracy. We expect that by using transfer learning, online learning can be performed in an unmeasured environment.
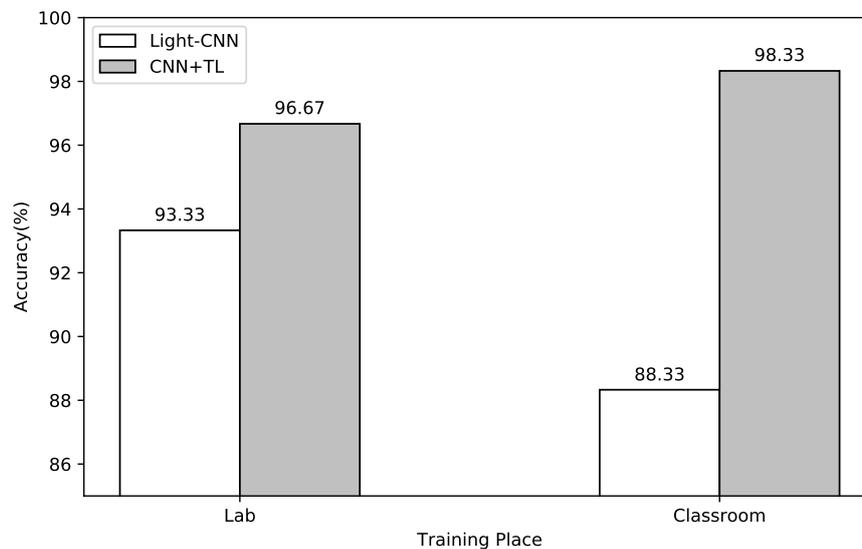

Figure 7. UWB channel classification accuracy of the light CNN and CNN with TL in different places.

Table 6. Training time comparison of different neural networks.

	MLP	CNN	MLP+TL	CNN+TL	Light-CNN
Lab	3 s	14 m 26 s	3 s	7 s	1 m 6 s
Classroom	4 s	14 m 28 s	3 s	18 s	1 m 22 s

6. Conclusions

As localization technologies using UWB are being commercialized, there have been active studies on UWB NLOS identification for high localization performance. Recently, many deep learning-based NLOS identification schemes have been proposed. However, there is a problem, in that performance seriously decreases in an unmeasured environment. To solve this problem, we proposed a transfer learning-based UWB NLOS identification scheme for an unmeasured environment. Experiments were conducted in both measured and unmeasured environments. In the measured environment, the proposed classifier models, MLP and CNN, showed an accuracy of up to 98.56% and 98.72%, respectively. In the unmeasured environment, the proposed transfer learning scheme showed an identification accuracy of up to 98.33% NLOS. This shows an accuracy improvement of approximately 55% and 48 times faster training compared to the CNN without transfer learning. Compared to training the new CNN model for an unmeasured environment, the proposed scheme shows a performance improvement of approximately 10% and an approximately five times faster learning speed. In short, the proposed method shows similar accuracy to the CNN trained with 30 times the data and a 48 times faster training time.

To operate transfer learning online, future research will need to be conducted to detect environmental changes and transfer learning without the data labeling process. In addition, we will focus on NLOS identification and NLOS error mitigation. The various lessons learned from this study will help in our future research.

Author Contributions: Conceptualization and methodology, J.P.; validation, Y.K. and Y.-B.K.; data curation and formal analysis, S.N. and H.C.; writing, original draft preparation, J.P. and H.C.; writing, review and editing, Y.K. and Y.-B.K.; supervision, Y.-B.K. All authors read and agreed to the published version of the manuscript.

Conflicts of Interest: The authors declare no conflict of interest.

References

1. Desk, E.D. Continental smartphone-based car key to be introduced in 2021 models of three more car manufacturers. *The Financial Express*, 24 January 2020. Available online: https://www.financialexpress.com/auto/car-news/continental-smartphone-based-car-key-cosma-2021-models-digital-car-key-apple/2002031 (accessed on 2 September 2020).

2. Eadicicco, L. Apple and Samsung newest phones use a little-known technology that lets your phone understand exactly where it is—And could mean you never misplace anything again. *Business Insider*, 20 August 2020. Available onlie: https://www.businessinsider.com/uwb-explained-samsung-galaxy-note-ultra-apple-iphone-features-airdrop-2020-8 (accessed on 2 September 2020).

3. Sedlacek, P.; Slanina, M.; Masek, P. An overview of the IEEE 802.15.4z standard its comparison and to the existing UWB standards. In Proceedings of the 2019 29th International Conference Radioelektronika (RADIOELEKTRONIKA), Pardubice, Czech Republic, 16–18 April 2019; pp. 1–6.

4. Gezici, S.; Tian, Z.; Giannakis, G.B.; Kobayashi, H.; Molisch, A.F.; Poor, H.V.; Sahinoglu, Z. Localization via ultra-wideband radios: a look at positioning aspects for future sensor networks. *IEEE Signal Process. Mag.* **2005**, *22*, 70–84. [CrossRef]

5. Connell, C. What's the difference between measuring location by UWB Wi-Fi and bluetooth? *Electron. Des. Febr.* **2015**, *6*, 2015. Available online: https://www.electronicdesign.com/technologies/communications/article/21800581/whats-the-difference-between-measuring-location-by-uwb-wifi-and-bluetooth (accessed on 7 October 2020).

6. Monica, S.; Ferrari, G. Improving UWB-based localization in IoT scenarios with statistical models of distance error. *Sensors* **2018**, *18*, 1592. [CrossRef] [PubMed]

7. Aileni, R.M.; Suciu, G.; Sukuyama, C.A.V.; Pasca, S.; Maheswar, R. Internet of wearable low-power wide-area network devices for health self-monitoring. In *LPWAN Technologies for IoT and M2M Applications*; Elsevier: London, UK, 2020; pp. 307–325.

8. Choi, H.B.; Lim, K.W.; Ko, Y.B. Sensor Localization System for AR-assisted Disaster Relief Applications (poster). In Proceedings of the 17th Annual International Conference on Mobile Systems, Applications, and Services, Seoul, Korea, 12–21 June 2019; pp. 526–527.

9. Ridolfi, M.; Vandermeeren, S.; Defraye, J.; Steendam, H.; Gerlo, J.; De Clercq, D.; Hoebeke, J.; De Poorter, E. Experimental evaluation of UWB indoor positioning for sport postures. *Sensors* **2018**, *18*, 168. [CrossRef] [PubMed]

10. Huo, Y.; Dong, X.; Beatty, S. Cellular Communications in Ocean Waves for Maritime Internet of Things. *IEEE Internet Things J.* **2020**, *7*, 9965–9979. [CrossRef]

11. Li, L.; Ren, H.; Cheng, Q.; Xue, K.; Chen, W.; Debbah, M.; Han, Z. Millimeter-wave networking in sky: A machine learning and mean field game approach for joint beamforming and beam-steering. *IEEE Trans. Wirel. Commun.* **2020**, *19*, 6393–6408. [CrossRef]

12. He, Y.; Chen, Y.; Hu, Y.; Zeng, B. WiFi Vision: Sensing, Recognition, and Detection with Commodity MIMO-OFDM WiFi. *IEEE Internet Things J.* **2020**, *7*, 8296–8317. [CrossRef]

13. Huo, Y.; Dong, X.; Lu, T.; Xu, W.; Yuen, M. Distributed and multilayer UAV networks for next-generation wireless communication and power transfer: A feasibility study. *IEEE Internet Things J.* **2019**, *6*, 7103–7115. [CrossRef]

14. Khodjaev, J.; Park, Y.; Malik, A.S. Survey of NLOS identification and error mitigation problems in UWB-based positioning algorithms for dense environments. *Ann. Telecommun./Annales des Télécommunications* **2010**, *65*, 301–311. [CrossRef]

15. Yu, K.; Wen, K.; Li, Y.; Zhang, S.; Zhang, K. A novel NLOS mitigation algorithm for UWB localization in harsh indoor environments. *IEEE Trans. Veh. Technol.* **2018**, *68*, 686–699. [CrossRef]

16. Kim, D.H.; Kwon, G.R.; Pyun, J.Y.; Kim, J.W. NLOS Identification in UWB channel for Indoor Positioning. In Proceedings of the 2018 15th IEEE Annual Consumer Communications & Networking Conference (CCNC), Las Vegas, NV, USA, 12–15 Janaury 2018; pp. 1–4.

17. Zeng, Z.; Bai, R.; Wang, L.; Liu, S. NLOS identification and mitigation based on CIR with particle filter. In Proceedings of the 2019 IEEE Wireless Communications and Networking Conference (WCNC), Marrakesh, Morocco, 15–18 April 2019; pp. 1–6.

18. Gururaj, K.; Rajendra, A.K.; Song, Y.; Law, C.L.; Cai, G. Real-time identification of NLOS range measurements for enhanced UWB localization. In Proceedings of the 2017 International Conference on Indoor Positioning and Indoor Navigation (IPIN), Sapporo, Japan, 18–21 Septemper 2017; pp. 1–7.

19. Zeng, Z.; Liu, S.; Wang, L. UWB NLOS identification with feature combination selection based on genetic algorithm. In Proceedings of the 2019 IEEE International Conference on Consumer Electronics (ICCE), Las Vegas, NV, USA, 11–13 Janaury 2019; pp. 1–5.

20. Kristensen, J.B.; Ginard, M.M.; Jensen, O.K.; Shen, M. Non-Line-of-Sight Identification for UWB Indoor Positioning Systems using Support Vector Machines. In Proceedings of the 2019 IEEE MTT-S International Wireless Symposium (IWS), Guangzhou, China, 19–22 May 2019; pp. 1–3.

21. Barral, V.; Escudero, C.J.; García-Naya, J.A. NLOS Classification Based on RSS and Ranging Statistics Obtained from Low-Cost UWB Devices. In Proceedings of the 2019 27th European Signal Processing Conference (EUSIPCO), Coruna, Spain, 2–6 September 2019; pp. 1–5.

22. Zeng, H.; Xie, R.; Xu, R.; Dai, W.; Tian, S. A Novel Approach to NLOS Identification for UWB Positioning Based on Kernel Learning. In Proceedings of the 2019 IEEE 19th International Conference on Communication Technology (ICCT), Xi'an, China, 16–19 October 2019; pp. 451–455.

23. Fan, J.; Awan, A.S. Non-line-of-sight identification based on unsupervised machine learning in ultra wideband systems. *IEEE Access* **2019**, *7*, 32464–32471. [CrossRef]

24. Wang, F.; Xu, Z.; Zhi, R.; Chen, J.; Zhang, P. Los/nlos channel identification technology based on cnn. In Proceedings of the 2019 6th NAFOSTED Conference on Information and Computer Science (NICS), Hanoi, Vietnam, 12–13 December 2019; pp. 200–203.

25. Stahlke, M.; Kram, S.; Mutschler, C.; Mahr, T. NLOS Detection using UWB Channel Impulse Responses and Convolutional Neural Networks. In Proceedings of the 2020 International Conference on Localization and GNSS (ICL-GNSS), Tampere, Finland, 2–4 June 2020; pp. 1–6.

26. ShirinAbadi, P.A.; Abbasi, A. Uwb channel classification using convolutional neural networks. In Proceedings of the 2019 IEEE 10th Annual Ubiquitous Computing, Electronics & Mobile Communication Conference (UEMCON), New York, NY, USA, 10–12 October 2019; pp. 1064–1068.

27. Jiang, C.; Shen, J.; Chen, S.; Chen, Y.; Liu, D.; Bo, Y. UWB NLOS/LOS Classification Using Deep Learning Method. *IEEE Commun. Lett.* **2020**, *24*, 2226–2230. [CrossRef]

28. Molisch, A.F.; Balakrishnan, K.; Chong, C.C.; Emami, S.; Fort, A.; Karedal, J.; Kunisch, J.; Schantz, H.; Schuster, U.; Siwiak, K. IEEE 802.15.4a channel model-final report. *IEEE P802* **2004**, *15*, 0662.

29. Decawave. EVK1000 User Manual. 2016. Available online: https://www.decawave.com/product/evk1000-evaluation-kit/ (accessed on 7 October 2020).

Publisher's Note: MDPI stays neutral with regard to jurisdictional claims in published maps and institutional affiliations.